



HAL
open science

Coherently controlled ionization of gases by three-color femtosecond laser pulses

Shixiang Wang, Chenhui Lu, Zhengquan Fan, Aurélien Houard, Vladimir Tikhonchuk, André Mysyrowicz, Songlin Zhuang, Vasily Kostin, Yi Liu

► **To cite this version:**

Shixiang Wang, Chenhui Lu, Zhengquan Fan, Aurélien Houard, Vladimir Tikhonchuk, et al.. Coherently controlled ionization of gases by three-color femtosecond laser pulses. *Physical Review A*, 2022, 105 (2), pp.023529. 10.1103/PhysRevA.105.023529 . hal-03593257

HAL Id: hal-03593257

<https://ensta-paris.hal.science/hal-03593257v1>

Submitted on 1 Mar 2022

HAL is a multi-disciplinary open access archive for the deposit and dissemination of scientific research documents, whether they are published or not. The documents may come from teaching and research institutions in France or abroad, or from public or private research centers.

L'archive ouverte pluridisciplinaire **HAL**, est destinée au dépôt et à la diffusion de documents scientifiques de niveau recherche, publiés ou non, émanant des établissements d'enseignement et de recherche français ou étrangers, des laboratoires publics ou privés.

Coherently controlled ionization of gases by three-color femtosecond laser pulses

Shixiang Wang,^{1,+} Chenhui Lu,^{2,+} Zhengquan Fan,¹ Aurélien Houard,³ Vladimir Tikhonchuk,^{4,5}

André Mysyrowicz,³ Songlin Zhuang,¹ Vasily A. Kostin,^{6,7,#} Yi Liu^{1,8,*}

¹ Shanghai Key Lab of Modern Optical System, University of Shanghai for Science and Technology, Engineering Research Center of Optical Instrument and System, The Ministry of Education, 516, Jungong Road, 200093 Shanghai, China

² School of Mechanical and Automotive Engineering, Shanghai University of Engineering Science, Shanghai, 201620, China

³ Laboratoire d'Optique Appliquée, ENSTA Paris, CNRS, Ecole Polytechnique, Institut Polytechnique de Paris, 828 Boulevard des Maréchaux, 91762 Palaiseau cedex, France

⁴ Centre Lasers Intenses et Applications, Université de Bordeaux – CNRS – CEA, 351 Cours de la Libération, 33405 Talence, France

⁵ ELI-Beamlines Center, Institute of Physics, Czech Academy of Sciences, 25241 Dolní Břežany, Czech Republic

⁶ Institute of Applied Physics, Russian Academy of Sciences, Nizhny Novgorod 603950, Russia

⁷ Scientific and Educational Mathematical Center, University of Nizhny Novgorod, Nizhny Novgorod 603950, Russia

⁸ CAS Center for Excellence in Ultra-Intense Laser Science, Shanghai 201800, China

#vk1@ipfran.ru, *yi.liu@usst.edu.cn

Abstract

Photoionization of atoms and molecules by intense femtosecond laser pulses is a fundamental process of strong-field physics. Using a three-color femtosecond laser scheme with attosecond phase control precision, we demonstrate coherently controlled ionization of nitrogen molecules with a modulation level up to 20% by varying the phase shifts between the fundamental laser frequency at 800 nm and its second and third harmonics. Furthermore, the phase dependence of the ionization degree qualitatively changes with the laser intensity ratios between the three colors. The observations are interpreted as a manifestation of the competition between different parametric channels contributing to the ionization process. Such coherent control of ionization opens new ways to finely tune and optimize various phenomena accompanying laser-material interactions: high-order harmonic and attosecond generation, nanofabrication, remote ablation of samples, and even guidance of discharge and control of lightning by lasers.

Photoionization of atoms and molecules lays the foundation for strong-field physics effects including the generation of high-order harmonics (HHG) and attosecond pulses [1], long-distance filamentary propagation [2], emission of microwave to terahertz (THz) electromagnetic waves [3,4], non-sequential double ionization and frustrated ionization [5-7], *etc.* For all these effects, the ionization rate and the corresponding final electron density are key parameters, and therefore, their proper control is highly desirable. With a single-color pulse, adaptive temporal pulse shape control has the capacity to enhance or suppress ionization of certain atoms or molecules, a process that is usually based on energy level resonance [8-12]. Moreover, it has been demonstrated that ionization of molecules can be enhanced and coherently controlled with two-color laser pulses composed of a fundamental frequency with either its second or third harmonics [13-15]. Recently, it has been reported that a laser field composed of 3 or more colors can be even more beneficial [16-18]. Compared to two-color laser field excitation, the three-color scheme provides extra control parameters and has proven its versatility in the selection of single harmonic radiation from the comb of high-order harmonics [19], in the coherent control of the polarization and chirality of THz pulses produced from air plasma [18], and in the generation of supercontinuum ranging from mid-infrared to ultraviolet [17,20]. However, the fundamental process of molecule ionization by a phase-controlled three-color laser field has remained largely unexplored.

In the present study, we demonstrate both experimentally and theoretically, using ambient air as an example, that the tunnel ionization of molecular gases can be coherently controlled by laser pulses composed of the fundamental frequency and its second and third harmonics. We find that the ionization degree of the formed plasma, monitored by its fluorescence, changes periodically when the phase shifts between the three harmonics are varied. Interestingly, it is also found that the ionization rate presents different dependences on the phases for different intensity ratios between the three colors of the laser field. The interpretation of the experimental results is based on the concept that different ionization channels contribute to electron tunneling in strong multicolor fields. The competition between the three different parametric channels is manifested through the complex phase dependences of the ionization rate. For different intensity ratios between the three colors, the dominating parametric channels of ionization changes, in agreement with the experimentally observed intensity-dependent phase graphs. These findings provide a robust and simple method for enhancing and controlling the ionization of atoms and molecules, which is of great significance for strong-field physics as well as nonlinear optics.

We used an in-line three-color femtosecond laser pulse to create a plasma filament in ambient air. The three-color pulse is composed of a fundamental field at 800 nm and its second and third harmonics. The relative phase $\Delta\phi$ between the fundamental pulse and the second harmonic pulse and that between the second harmonic and third harmonic ($\Delta\gamma$) can be precisely controlled by displacement of a fused silica wedge and BBO 2. The experimental setup is shown in Fig. 1. The details of the setup and the polarization status of the pulses can be found in the Supplemental Materials.

A typical emission spectrum of the air plasma filament is shown in Fig. 2 (a). The observed lines correspond to transitions between excited triplet states $C^3\Pi_u^+$ and $B^3\Pi_g^+$ of neutral nitrogen molecules (the 2nd positive system of N_2) and between the second excited state $B^2\Sigma_u^+$ and ground state $X^2\Sigma_g^+$ of nitrogen molecular ions (the 1st negative system of N_2^+) [21]. In Fig. 2 (a), the corresponding transitions are indicated. The emission of nitrogen ions at 391.4 nm corresponds to the electronic transition from the HOMO-2 orbital to the highest occupied molecular orbital (HOMO). Therefore, its spectral intensity reflects the population density of nitrogen ions in the $B^2\Sigma_u^+$ state. Regarding the emission from neutral nitrogen molecules, it is known that the upper molecular state $C^3\Pi_u^+$ becomes occupied through collisional excitation of nitrogen molecules in the ground state $X^1\Sigma_g^+$ with energetic electrons [21,22]. Therefore, the corresponding line intensities are linearly proportional to the electron density inside the plasma, proportional to the ionization of oxygen molecule since its energy bandgap is smaller than that of nitrogen molecules. Here, we select the 337 nm and 391.4 nm lines for monitoring, which represent the production of free electrons and nitrogen ions, respectively.

In Fig. 2 (b), we present the dependence of the 391.4 and 337 nm signals when the optical wedge thickness is continuously increased in the optical beam path. Positive delay corresponds to a 400 nm pulse arriving after the 800 nm pulse. The signals increase and decrease upon scanning of the optical wedge, reflecting the transitory temporal overlap of the 800 nm and 400 nm pulses, which results in third harmonic generation at 266 nm. More importantly, a modulation with a period of ~ 1.3 fs is noticeable, which indicates coherent ionization control determined by the phase $\Delta\phi$ between 800 and 400 nm. A maximum modulation depth of $\sim 20\%$ is routinely observed in the experiments. For comparison, we also presented the results obtained with 800 and 400 nm laser fields, where the modulation is barely observable. This demonstrated the advantageous

of the three-color fields compared with the two-color case. The Fourier transformation of the signals in three-color pumping in Fig. 2 (b) is presented in Fig. 2 (c). This transformation yields a main peak at 0.75 PHz (corresponding to the temporal period of 1.3 fs or the period 2π in phase $\Delta\varphi$) and a secondary peak at 1.49 PHz (corresponding to the temporal period 0.67 fs or the phase period of π). Their origin will be discussed later.

We then investigated the influence of both $\Delta\varphi$ and $\Delta\gamma$ on the ionization rate. In the experiments, different laser intensity ratios of the three optical frequencies were examined. To study the effect of relative intensity changes between the three optical fields at 800, 400, and 266 nm, we performed measurements of the plasma fluorescence a) at different locations along the long filament (point A or B in Fig. 1), b) by changing the partial or total temporal overlap between the three colors (Fig. 2 (b)), or c) by changing the incident 800 nm pulse energy. The fluence and corresponding averaged laser intensity of the three optical fields inside the filaments were calculated using the method involving an in situ filament-drilled pinhole, which provides a measurement of the average laser fluence within a diameter of $\sim 90 \mu\text{m}$ in the current experiments [23,24]. The measured diameter of the filament-drilled pinhole and the laser fluence of the three wavelengths are summarized in the [Supplemental Material](#).

In the first experiment, we measured the fluorescence at the front of the plasma (location A in Fig. 1) with a partial overlap of the 400 nm pulses with the main 800 nm pulses (stage I in Fig. 2 (b)). The ratio of intensities $I^{(400)}/I^{(800)}$ was then estimated to be 0.049. The measured dependence of the 337 nm signal on both $\Delta\varphi$ and $\Delta\gamma$ is shown in Fig. 3 (a) in the form of a 2D phase diagram. The corresponding result for the 391.4 nm fluorescence is presented in Fig. S1 (a). Here, the maximum ionization signal remains approximately constant, and the peaks in the 2D phase diagram shift continuously upon an increase in both $\Delta\varphi$ and $\Delta\gamma$. In other words, a constant $\Delta\varphi + \Delta\gamma$ gives rise to a rather constant ionization rate. We next moved to the middle of the filament (location B in Fig. 1) and performed the measurement around a good temporal overlap between the 400 and 800 nm pulses (stage II in Fig. 2 (b)). In this case, the incident 800 nm pulse energy was 0.65 mJ. The intensity ratio $I^{(400)}/I^{(800)}$ was estimated to be 0.163. The corresponding results for 337 nm and 391.4 nm fluorescence are presented in Fig. 3 (b) and Fig. S2 (b). Here, the maximum ionization is achieved at some isolated regions in the 2D phase diagram; *i.e.*, a “chessboard” pattern is observed. In the third case, the intensity ratio $I^{(400)}/I^{(800)}$ was further increased to 0.397 by increasing the incident 800 nm pulse energy to 1.88 mJ. The corresponding results are shown in Fig. 3 (c) and Fig. S1 (c). Now, the maximum ionization remains rather constant again, while the peaks shift gradually for a constant $\Delta\varphi - \Delta\gamma$. To obtain further insight into the 2D phase dependence of Fig. 3 and Fig. S2, we performed 2D Fourier transformation. The corresponding results are shown in Fig. 4 and Fig. S3. A series of peaks are observed in the frequency map, with different peaks dominating the three regions of the intensity ratio $I^{(400)}/I^{(800)}$. As will be discussed, these peaks correspond to the different parametric channels involved for tunneling ionization.

To explain the results of the experiment, we calculated the plasma density produced in the tunnel ionization of gas molecules by the three-color linearly polarized electric field $\mathbf{E}(t) = E(t)\hat{\mathbf{x}}$,

$$E(t) = F(t) \left[E_{800} \cos(\omega_{800}t) + E_{400} \cos(2\omega_{800}t + \varphi) + E_{266} \cos(3\omega_{800}t + \varphi + \gamma) \right]. \quad (1)$$

Here, $F(t) = e^{-2\ln 2(t/\tau_p)^2}$ is the pulse envelope, τ_p is the intensity full-width at half-maximum,

$E_{800,400,266} = \sqrt{2I^{(800,400,266)}/c\epsilon_0}$ are the peak amplitudes of the fundamental, second, and third harmonics,

$I^{(800,400,266)}$ are their peak intensities, c is the speed of light, ε_0 is the vacuum permittivity, $\omega_{800} = 2\pi c/\lambda_{800}$ is the fundamental frequency, φ is the phase shift between the second and fundamental harmonics, and γ is the phase shift between the third and second harmonics. The time-varying plasma density $N(t)$ satisfies the ionization equation $\partial N/\partial t = (N_g - N)w(|E|)$ with zero initial condition at time $t \rightarrow -\infty$, where N_g is the initial concentration of neutral particles, and $w(|E|)$ is the tunnel ionization probability per unit time in the static electric field.

Using the multiwave mixing approach from [28], one can find the analytical expression for the period-averaged ionization probability

$$\bar{w}(t) \approx \sum_{r=0}^{\infty} \sum_{s=-\infty}^{\infty} (2 - \delta_{r0}) W_{[3r+4s], 2|s|, |r|}(t) \cos(r\gamma + (r+2s)\varphi), \quad (2)$$

where δ_{jk} is the Kronecker delta and $W_{pqr}(t)$ are the slow coefficients defined by the intensities of the three colors. The detailed derivation of (2) and the expressions for W_{pqr} are given in the [Supplemental Materials](#). Each term in sum (2) corresponds to a different parametric channels of ionization [28,29], that is, to a different way to represent zero frequency as a combination of frequencies ω_{800} , $2\omega_{800}$, and $3\omega_{800}$ with an odd sum of coefficients. Since the coefficients W_{pqr} decrease quickly with their indices, only a few terms in (2) contribute significantly to the period-averaged ionization rate. If the third harmonic is not too small so that $W_{4,2,0} \ll W_{1,2,1} + W_{3,0,1}$, only three parametric channels provide the main contributions, *i.e.*, (i) $r=0, s=0$; (ii) $r=1, s=0$; and (iii) $r=1, s=-1$, which gives

$$\bar{w} \approx W_{0,0,0} + 2W_{3,0,1} \cos(\varphi + \gamma) + 2W_{1,2,1} \cos(\varphi - \gamma). \quad (3)$$

Equation (3) describes well both the phase dependences observed in our experiments and the transitions between them when changing the intensity ratio $I^{(400)}/I^{(800)}$. The first term in Eq. (3) describes the main channel of ionization, which is present even without the second and third harmonics and does not depend on their phases. The second term is associated with joint ionization by the fundamental and third harmonics, whereas the third term requires the presence of all three colors and depends significantly on the amplitude of the second harmonic in contrast to the first two terms. Therefore, the ratio between the amplitudes of the second and third terms depends significantly on the ratio $I^{(400)}/I^{(800)}$: for a relatively weak second harmonic (with $I^{(400)}/I^{(800)}$ less than some critical value of approximately 1/4), $W_{3,0,1} > W_{1,2,1}$ holds and the 2D phase dependence is tilted left as shown in [Fig. 3 \(a\) and 4 \(a\)](#); for the strong second harmonics, $W_{3,0,1} < W_{1,2,1}$, the phase dependence is tilted right as in [Fig. 3 \(c\) and 4 \(c\)](#).

Note that if the third harmonic is absent or small enough so that $W_{4,2,0} \gg W_{1,2,1} + W_{3,0,1}$, then the ionization rate becomes almost independent of γ , whereas the dependence on φ is defined by the parametric channels with $r=0, s=\pm 1$ in sum (2), $\bar{w} \approx W_{0,0,0} + 2W_{4,2,0} \cos 2\varphi$. It is interesting that in this case, the ionization rate is π -periodic with respect to φ (which is manifested as the peak at 1.43 PHz in [Fig. 2\(c\)](#)), in contrast to the prediction of Eq. (3) for the strong third harmonic where the period should be 2π . This period doubling originates from breaking the mirror symmetry of the two color fields containing only the fundamental and second harmonics due to the addition of the third harmonic. This effect is very similar to the period doubling that occurs in the phase dependence of the amplitude of THz radiation generated by the three-color pulse [18].

We also solved the ionization equation numerically and calculated the final ionization degree

$\sigma_f = N(t \rightarrow +\infty)/N_g$ created by the three-color field (1). In the calculations below, we use the formula in Refs. [13,16,18,25] for the ionization rate of the molecular nitrogen, $w(|E|) = 4\omega_a \kappa^5 (E_a/|E|) \exp(-2\kappa^3 E_a/3|E|)$, where $\omega_a \approx 4.13 \cdot 10^{16} \text{ s}^{-1}$ and $E_a \approx 5.14 \cdot 10^9 \text{ V/cm}$ are the atomic units of frequency and field strength, respectively, and $\kappa = \sqrt{U_{N_2}/U_H}$, with $U_H = 13.6 \text{ eV}$ and $U_{N_2} = 15.6 \text{ eV}$ being the ionization potentials of atomic hydrogen and molecular nitrogen, respectively.

The dependences of σ_f on phases φ and γ are presented in Fig. 5 and are consistent with both the experimental results presented in Fig. 3 and the analytical Eqs. (2) and (3). In Fig. 5(d), we also presented the simulation results for two-color fields containing 800 and 400 nm fields. The ionization modulation is much less than the three-color excitation, in agreement with the experimental observation in Fig. 2 (b). Figure S3 shows the calculated variation in σ_f with phases φ and γ (difference between maximum and minimum over phases) as a function of $I^{(400)}$ and $I^{(266)}$. The variation may reach tens of percent, resulting in a strong enhancement or suppression of ionization. The comparison of the first and second term in Eq. (3) and the calculation results presented in Fig. S4 show that the relative variation in the ionization rate due to the presence of the third harmonic becomes significant for relatively weak 266 nm fields when $E_{266}/E_{800} \sim 3E_{800}/2\kappa^3 E_a$. It should also be noted that the presence of the second harmonic itself (without the third harmonic) does not result in substantial variation in the ionization rate since it is defined by weak parametric channels $r=0$, $s=\pm 1$. However, the second harmonic can significantly enhance the control effect from the third harmonic (as is also seen in Fig. S4), which makes the three-color pulses containing both the second and third harmonics more advantageous for coherent ionization control than the two-color pulses.

In summary, we investigated the ionization of gas molecules in air by an intense femtosecond laser field consisting of a fundamental frequency and second and third harmonics. It was found that the ionization rates of both the HOMO and the HOMO-2 of nitrogen molecules depend sensitively on the relative phases between the three colors. For different intensity ratios between the 400 nm and 800 nm pulses, the ionization shows a different dependence on the two phases, manifesting as 2D “strips” tilted left or right. We simulated the ionization process driven by multiple color laser fields in the tunnel regime and revealed that the ionization rate is determined by a series of multiple-wave mixing terms (parametric channels of ionization). Depending on the relative strength of the laser fields, the maximum ionization rate can be dominated by different wave mixing terms, in good agreement with our experimental observations. The control of strong field ionization rates by a three-color scheme is general and can be applied to other atomic and molecular gases in addition to air. Therefore, the possibility of controlling the ionization rate by changing the phase structure of the ionizing field opens new ways to control and optimize laser–material interactions.

References:

- [1] M. Hentschel, *et al*, Attosecond metrology, *Nature* **414**, 509 (2001).
- [2] A. Couairon and A. Mysyrowicz, Femtosecond filamentation in transparent media, *Phys. Rep.* **441**, 47 (2007).
- [3] X. Xie, J. Dai, and X.-C. Zhang, Coherent control of THz wave generation in ambient air, *Phys. Rev. Lett.* **96**, 075005 (2006).
- [4] A. Mitrofanov, *et al*, Coherently enhanced microwave pulses from midinfrared-driven laser plasmas, *Opt. Lett.* **46**, 1081 (2021).

- [5] B. Bergures, et al, Attosecond tracing of correlated electron-emission in non-sequential double ionization, Nat. Commun. **3**, 813 (2012).
- [6] T. Nubbemeyer, K. Gorling, A. Saenz, U. Eichmann, W. Sandner, Strong-field tunneling without ionization, Phys. Rev. Lett. **101**, 233001 (2008)
- [7] Y. Zhao, *et al*, Frustrated tunneling ionization in the elliptically polarized strong laser fields, Opt. Express, **27**, 21689 (2019).
- [8] E. Papastathopoulos, M. Strehle, and G. Gerber, Optimal control of femtosecond multiphoton double ionization of atomic calcium, Chem. Phys. Lett. **408**, 65 (2005).
- [9] L. Englert, *et al*, Control of ionization processes in high band gap materials via tailored femtosecond pulses, Opt. Express **15**, 17855 (2007).
- [10] A. Castro, E. Räsänen, A. Rubio, and E. Gross, Femtosecond laser pulse shaping for enhanced ionization, Europhys. Lett. **87**, 53001 (2009).
- [11] J. Plenge, *et al*, Coherent control of the ultrafast dissociative ionization dynamics of bromochloroalkanes, Phys. Chem. Chem. Phys. **13**, 8705 (2011).
- [12] N. Shvetsov-Shilovski, L. Madsen, and E. Räsänen, Suppression of strong-field ionization by optimal pulse shaping: Application to hydrogen and the hydrogen molecular ion, Phys. Rev. A **91**, 023425 (2015).
- [13] D. Schumacher and P. Bucksbaum, Phase dependence of intense-field ionization, Phys. Rev. A **54**, 4271 (1996).
- [14] P. Béjot, *et al*, Harmonic generation and nonlinear propagation: when secondary radiations have primary consequences, Phys. Rev. Lett. **112**, 203902 (2014).
- [15] D. Jang, *et al*, Efficient terahertz and Brunel harmonic generation from air plasma via mid-infrared coherent control, Optica **6**, 1338 (2019).
- [16] P. González. de Alaiza Martínez, *et al*, Boosting terahertz generation in laser-field ionized gases using a sawtooth wave shape, Phys. Rev. Lett. **114**, 183901 (2015).
- [17] V. A. Kostin and N. V. Vvedenskii, Generation of few-and subcycle radiation in midinfrared-to-deep-ultraviolet range during plasma production by multicolor femtosecond pulses, Phys. Rev. Lett. **120**, 065002 (2018).
- [18] S. Liu, *et al*, Coherent control of boosted terahertz radiation from air plasma pumped by a femtosecond three-color sawtooth field, Phys. Rev. A **102**, 063522 (2020).
- [19] P. Wei, *et al*, Selective enhancement of a single harmonic emission in a driving laser field with subcycle waveform control, Phys. Rev. Lett. **110**, 233903 (2013).
- [20] Y. Kida, K. Sakamoto, and T. Imasaka, High-energy multicolor femtosecond pulses in the deep-ultraviolet generated through four-wave mixing induced by three-color pulses, App. Phys. B **122**, 214 (2016).
- [21] S. Mitryukovskiy, *et al*, Plasma Luminescence from Femtosecond Filaments in Air: Evidence for Impact Excitation with Circularly Polarized Light Pulses, Phys. Rev. Lett. **114**, 063003 (2015).
- [22] R. Danylo, *et al*, Formation Dynamics of Excited Neutral Nitrogen Molecules inside Femtosecond Laser Filaments, Phys. Rev. Lett. **123**, 243203 (2019).
- [23] S. I. Mitryukovskiy, Y. Liu, A. Houard, and A. Mysyrowicz, Re-evaluation of the peak intensity inside a femtosecond laser filament in air, J. Phys. B: At. Mol. Opt. Phys. **48**, 094003 (2015).
- [24] H. Guo, *et al*, Direct measurement of radial fluence distribution inside a femtosecond laser filament core, Opt. Express **28**, 15529 (2020).
- [25] P. Corkum, N. Burnett, and F. Brunel, Above-threshold ionization in the long-wavelength limit, Phys. Rev. Lett. **62**, 1259 (1989).
- [26] X.-M. Tong, Z. Zhao, and C.-D. Lin, Theory of molecular tunneling ionization, Phys. Rev. A **66**, 033402 (2002).

- [27] Q. Zhang, *et al*, Sub-cycle coherent control of ionic dynamics via transient ionization injection, *Commun Phys* **3**, 1 (2020).
- [28] V. A. Kostin and N. V. Vvedenskii, Mutual enhancement of Brunel harmonics, *JETP Lett.* **110**, 457 (2019).
- [29] L. Li, *et al*, Scaling law of high harmonic generation in the framework of photon channels, *Phys. Rev. Lett.* **120**, 223203 (2018).

Acknowledgments

The work is supported in part by the National Natural Science Foundation of China (Grant Nos. 12034013, 11604205, 11904232), Innovation Program of Shanghai Municipal Education Commission (Grant No. 2017-01-07-00-07-E00007), and “The Belt and Road Initiative” international collaboration project of Shanghai Municipal Commission of Science and Technology (Grant No. 19560745800). C. Lu acknowledges support from the Talent Program of Shanghai University of Engineering Science. V. A. K. acknowledges support from the Russian Science Foundation (Grant No. 18-11-00210).

Figure 1

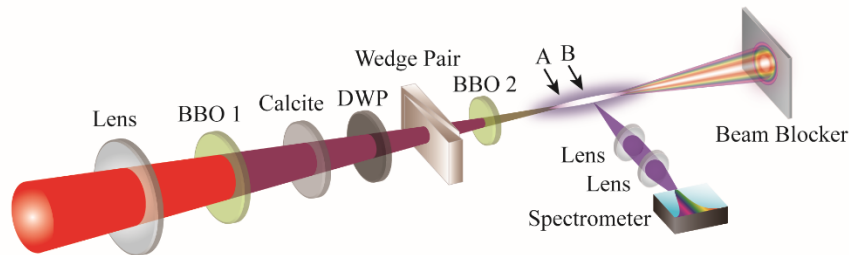


Fig. 1. Schematic experimental setup is presented. The details of the setup are presented in the Supplemental Materials. The fluorescence of the air plasma was collected by two lenses of $f = 20$ mm and 35 mm into the fiber tip and analyzed by a spectrometer. The two arrows indicate locations A and B, from where the fluorescence was collected and analyzed.

Figure 2

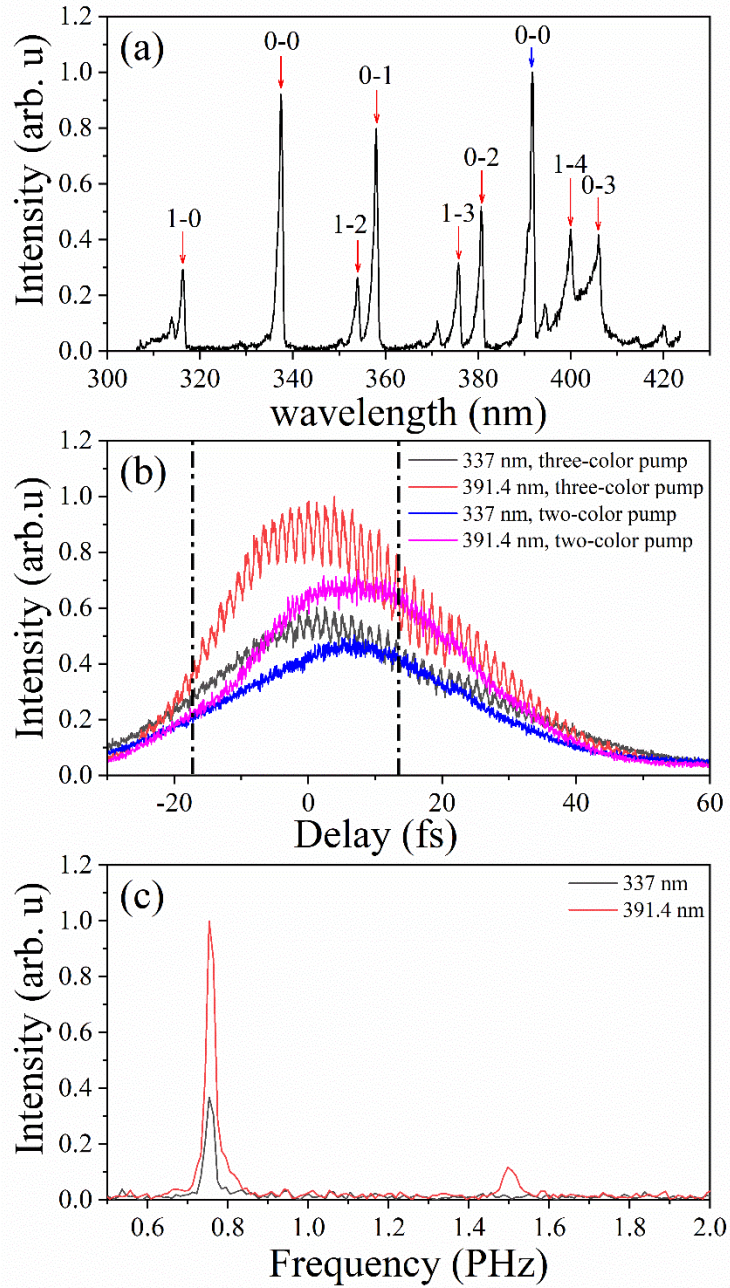


Fig. 2. (a) Emission spectrum of the air plasma. The spectral peaks stem from transitions between different energy levels of N_2 and N_2^+ . The related vibrational quantum numbers of the upper and lower levels of the 2nd positive band of N_2 (red arrow) and 1st negative band of N_2^+ (blue arrow) are indicated. (b) The 337 nm and 391.4 nm fluorescence as a function of the phase shift $\Delta\varphi$ between the second harmonic and fundamental field (proportional to the temporal delay $\Delta\tau$ introduced by the wedge pair), in case of two-color and three-color pumping. The pulse energy of the 800 nm pump laser is 1.8 mJ. (c) The Fourier transform of the signal obtained in three-color case in (b).

Figure 3

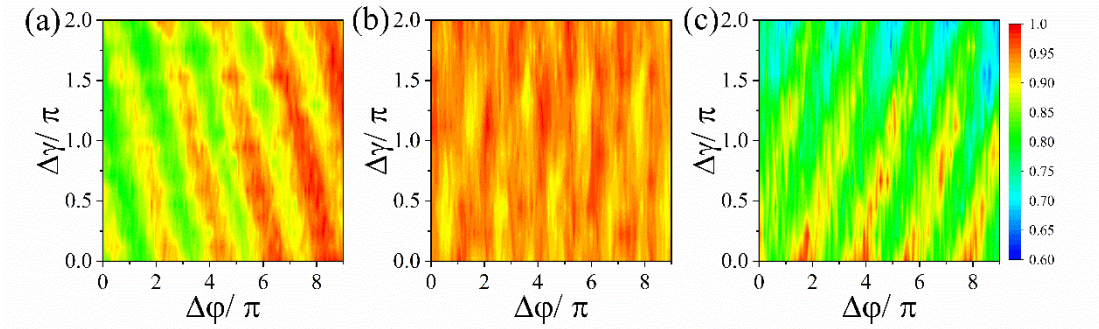


Fig. 3. Dependence of the 337 nm fluorescence signal on the relative phases $\Delta\varphi$ and $\Delta\gamma$. (a) The signals are collected at the front side of the plasma (location A in Fig. 1) and at the rising edge in Fig. 2 (b). The pump pulse energy is 1.88 mJ. (b) The signals are collected in the middle of the plasma (location B) and at the summit of Fig. 2 (b). The pump energy is 0.65 mJ. (c) The signals are collected at the front edge of the plasma (location A in Fig. 1) and at the summit of Fig. 2 (b). The pump pulse energy is 1.88 mJ.

Figure 4

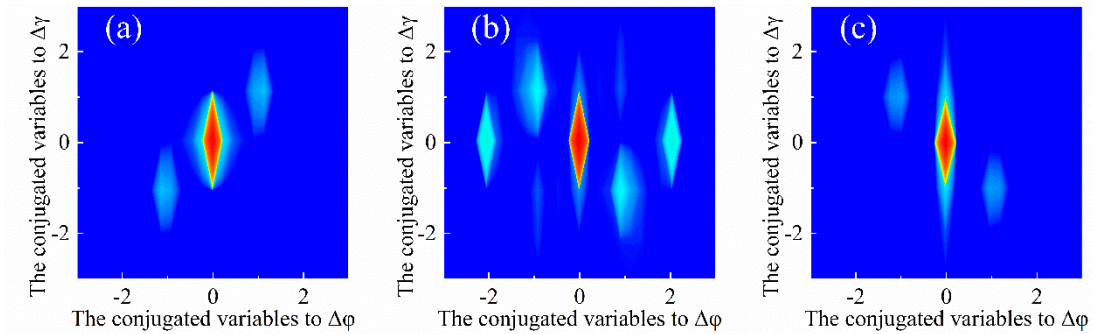


Fig. 4. The normalized 2D Fourier transform (logarithmic scale) of the experimental signals shown in Fig. 3.

Figure 5

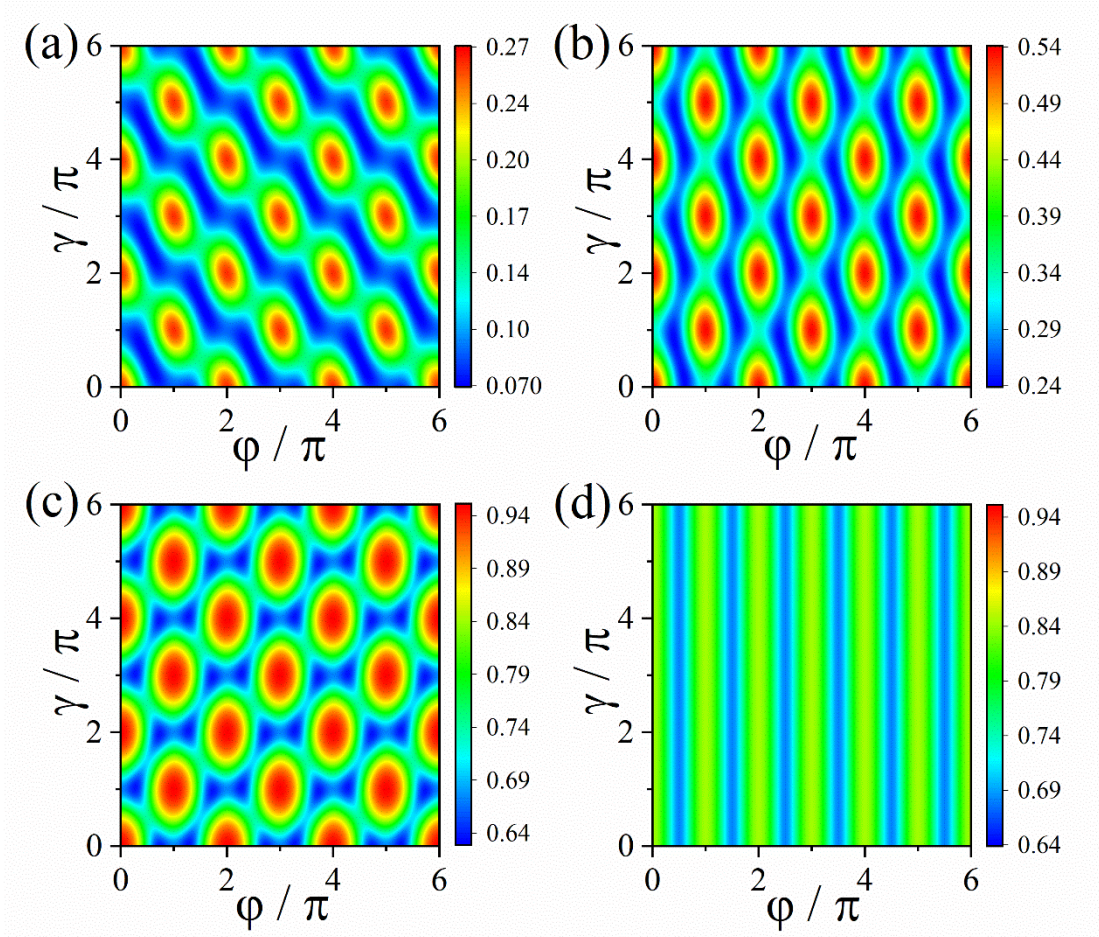


Fig. 5. Calculated ionization degree of nitrogen molecules as a function of the relative phases. (a)–(c) The intensity of the 800 nm laser field is 1.5×10^{14} W/cm², and the intensity ratios between the 800, 400, and 266 nm pulses are 1: 0.05: 0.008, 1: 0.16: 0.004, and 1: 0.4: 0.017 for (a), (b), and (c), respectively. In (d), the intensity of the 266 nm pulses is set to be 0 and the other parameters are the same as those of (c).